Title:

Phylogenetic incongruence and the origins of cardenolide-resistant forms of Na^+,K^+-ATPase in North American *Danaus* butterflies

Authors:

Matthew L. Aardema[1,2], Peter Andolfatto[1,3]

[1] Department of Ecology and Evolutionary Biology, Princeton University, Princeton, NJ, 08544, USA

[2] Current Address: American Museum of Natural History, New York, NY, 10024, USA

[3] Lewis-Sigler Institute for Integrative Genomics, Princeton University, Princeton, NJ, 08544, USA

Correspondence: Matthew L. Aardema

E-mail: maardema@amnh.org

Abstract

Rapid species radiations can obscure phylogenetic relationships between even distantly related species and lead to incorrect evolutionary inferences. For this reason, we examined evolutionary relationships among the three North American milkweed butterflies, *Danaus plexippus*, *D. gilippus* and *D. eresimus* using >400 orthologous gene sequences assembled from transcriptome data. Contrary to previous phylogenetic assessments, our results indicate that *D. plexippus* and *D. eresimus* are the sister taxa among these species. This result explains many previously noted phylogenetic incongruences such as an amino acid substitution in the sodium-potassium pump (Na^+,K^+-ATPase) of *D. eresimus* and *D. plexippus*, which increases resistance to the toxins found in these butterflies' host plants. In accordance with a rapid radiation of *Danaus* butterflies, we also find evidence that both incomplete lineage sorting and post-speciation genetic exchange have contributed significantly to the evolutionary histories of these species. Furthermore, our findings suggest that *D. plexippus* is highly derived both morphologically and behaviorally.

Key Words: *Danaus,* Danaidae, milkweed butterfly, incomplete lineage sorting, genetic introgression, Na^+,K^+-ATPase

Introduction

Plants in the genus *Asclepias* (milkweed) often produce a class of toxic, secondary metabolites called cardenolides, which provide defense against herbivory (Dobler et al. 2011; Agrawal et al. 2012). Despite these protective chemicals, many insect species have evolved the ability to feed on these plants. The phylogenetically broad insect herbivore community that specializes on *Asclepias* has proved to be a particularly good system for studying convergent evolution (Dobler et al. 2012; Zhen et al. 2012; Petschenka et al. 2013). Studies of convergence in these insects have improved our understanding of the underlying genetic architecture behind adaptive traits and given insights into the extent of constraint on genetic change (Stern 2013; Dobler et al. 2015).

As larvae, butterflies of the genus *Danaus* feed almost exclusively on *Asclepias* host plants (Ackery and Vane-Wright 1984). Many species also sequester the plants' toxins for their own defense (Brower and Moffit 1974; Ackery and Vane-Wright 1984). Within the three species of North American *Danaus*, both *D. plexippus* (the monarch) and *D. eresimus* (the soldier) appear to be fixed for a functionally important amino acid substitution in the H1-H2 extracellular domain of Na^+K^+-ATPase (N122H; Fig. S1; Zhen et al. 2012). This substitution decreases larval sensitivity to cardenolides consumed while feeding on *Asclepias* host plants, and may also facilitate toxin sequestration (Dobler et al. 2012; Zhen et al. 2012; Petschenka et al. 2013). The N122H substitution has not been observed in the third North American *Danaus*, *D. gilippus* (the queen; Holzinger and Wink 1996; Aardema et al. 2012; Dobler et al. 2012; Zhen et al. 2012; Petschenka et al. 2013).

58 Interestingly, among these three species, *D. gilippus* and *D. eresimus* have
59 historically been considered sister taxa, while *D. plexippus* has been classified as a
60 more distant relative within the *Danaus* genus (Fig. S1; Ackery and Vane-Wright
61 1984). This relationship was initially based on a large number of shared
62 morphological traits and behavioral similarities between *D. gilippus* and *D. eresimus*,
63 and it received further supported in analyses using sequence data from a small
64 number of mitochondrial (mtDNA), ribosomal (rRNA) and nuclear genes (Lushai et
65 al. 2003; Smith et al. 2005; Brower et al. 2010). However, in addition to the N122H
66 substitution shared by *D. eresimus* and *D. plexippus*, other apparent phylogenetic
67 incongruences have also been noted. For example, *D. eresimus* and *D. plexippus* are
68 each reported to have 30 chromosomes, whereas *D. gilippus* appears to typically
69 have 29 (Brown et al. 2004). Also, *D. eresimus* and *D. plexippus* have a shared Malic
70 enzyme (ME) allozyme phenotype distinct from *D. gilippus* (Kitching 1985). A third
71 example of apparent phylogenetic incongruence in these butterflies are the rear
72 projections on the eighth sternal segment of *D. eresimus* and *D. plexippus* males,
73 which *D. gilippus* males lack (Ackery and Vane-Wright 1984).

74 Given the inferred species phylogeny that places *D. gilippus* and *D. eresimus*
75 as closer relatives within *Danaus*, the origins of the N122H substitution and other
76 incongruences are unclear. In the case of N122H, it is possible that this mutation
77 arose independently and in parallel within both *D. plexippus* and *D. eresimus*, and
78 then subsequently fixed in each butterfly. Examples of this specific mutation
79 evolving in disparate taxa have been reported previously, in other insect taxa,
80 although not in other Lepidoptera outside the *Danaus* genus (Aardema et al. 2012;

Zhen et al. 2012). It is also possible that both the asparagine (N) and histidine (H) alleles were segregating in the common ancestor of these three species. If this is the case, then the histidine must have fixed independently in *D. plexippus* and *D. eresimus*, while being lost in *D. gilippus*. Such incomplete lineage sorting (ILS) is a common cause of phylogenetic incongruence (Degnan and Rosenberg 2006; 2009; Maddison and Knowles 2006). Adaptive introgression is a third hypothesis to explain fixation of the N122H allele in both *D. plexippus* and *D. eresimus*. Genetic exchange after splitting has become increasingly recognized as an important contributor to the evolutionary history of species (reviewed in Mallet et al. 2015), and it can often lead to phylogenetic incongruence (e.g. Bachtrog et al. 2006; Baack and Rieseberg 2007; Cui et al. 2013).

It is also possible that while the many morphological and behavioral similarities of *D. eresimus* and *D. gilippus* suggest they are more closely related, our understanding of the phylogenetic relationships of North American *Danaus* may benefit from a fresh examination. For this reason, the first goal of this study was to re-evaluate species relationships among these butterflies using a much larger set of genetic sequences than has previously been employed. We also compared the extent to which ILS and genetic introgression may have contributed to phylogenetic incongruences between these species. Both ILS and genetic introgression have previously been proposed to explain observed morphological and genetic incongruences in the *Danaus* genus (Lushai et al. 2003; Smith et al. 2005), but to date neither hypothesis has been examined explicitly.

Our results indicate that in contrast to previous phylogenetic analyses, *D. eresimus* and *D. plexippus* are the sister taxa among North American *Danaus* butterflies. This suggests that the N122H mutation in both species can be explained by an origin in their shared, common ancestor. However, we also find that levels of genetic incongruence in these species are high, and may result from both ILS and post-splitting genetic exchange. In addition to the origins if the N122H mutation in *Danaus*, the findings of this study indicate that *D. plexippus* is highly derived morphologically and behaviorally, relative to other *Danaus* species.

Materials and Methods

Data preparation and location of orthologous sequences

To examine phylogenetic incongruences and the origins of the N122H substitution within *Danaus*, we took advantage of previously produced RNAseq data for the three *Danaus* species present in North America and a fourth milkweed butterfly outgroup, *Lycorea halia* (Zhen et al. 2012). Using just three focal species allows us to compare a major topology to only two possible minor topologies in a series of four-taxa trees, and assess whether these minor topologies occur at similar or different frequencies to one another. Such an assessment is a common way to investigate the origins of phylogenetic incongruence (e.g. Green et al. 2010; Eriksson and Manica 2012).

Reference-mapped alignments

125 Raw RNAseq reads from each of the four species were trimmed for quality
126 (Phred QV ≥ 20) and contiguous length (≥ 30 nucleotides). We first mapped the
127 trimmed reads from each sample to *D. plexippus* reference coding sequences (CDS;
128 http://monarchbase.umassmed.edu/resource.html) using Stampy (v. 1.0.17; Lunter
129 and Goodson 2011) with default parameters except substitution rate, which we set
130 to 0.01. We used SAMtools (v. 0.1.4) to convert the resulting SAM formatted files to
131 BAM formatted files while filtering for mapping quality (MAPQ > 20, Li et al. 2009).
132 The MarkDuplicates utility in Picard tools (v. 1.77;
133 http://broadinstitute.github.io/picard/) was used to remove PCR duplicates. We
134 used the HaplotypeCaller utility in GATK (v. 3.3; McKenna et al. 2010) to call
135 variants, and then filtered all sites for a minimum read depth of 30. All sequences
136 were checked by eye to ensure indels were in frame with relation to the reference.
137
138 *De novo-assembled alignments*
139 For a second set of sequence alignments, we produced independent *de novo*
140 transcriptome assemblies for each species using the programs Velvet (v. 1.2.10) and
141 Oases (v. 0.2.08) with a kmer length of 31 and a minimum read depth of 10 (Zerbino
142 and Birney 2008; Schulz et al. 2012). In cases where multiple isoforms were
143 assembled, we retained only the longest one. We located mtDNA regions by blasting
144 each of the four species' transcripts against the *D. plexippus* mitochondrial genome
145 (Genbank accession number KC836923; 'blastn'; Altschul et al. 1990). This was done
146 for comparison to previously published results (Lushai et al. 2003; Smith et al. 2005;
147 Brower et al. 2010). To locate orthologous nuclear sequences from our assembled

148 transcriptomes, the four transcript sets were compared to amino acid sequences of
149 predicted proteins for *D. plexippus* (Dp_geneset_OGS2_pep.fasta,
150 http://monarchbase.umassmed.edu/resource.html), using Blast with a translated
151 nucleotide query ('blastx') and a minimum e value of 1e-50. We compared our
152 transcripts to amino acid sequences to improve likely ortholog recognition in the
153 outgroup, *L. halia*. Only Blast hits that were at least 100 nucleotides long were
154 retained for subsequent ortholog comparison between the four species. This was
155 done to reduce regions that had limited phylogenetic information in our dataset, as
156 well as improve the accuracy of our alignments (Talavera and Castresana 2007). For
157 regions where any species had more than one transcript matching the *D. plexippus*
158 reference protein sequence, we discarded this region for all species to avoid
159 potential gene duplicates. Generally, a low level of polymorphism within a sample
160 does not affect contig assembly in Velvet, and in these cases only a single allele is
161 retained (Zerbino and Birney 2008). However, it is possible that highly polymorphic
162 regions will assemble into more than one distinct transcript. In our pipeline, such
163 regions would resemble gene duplicates and subsequently be removed.

164 We aligned orthologous regions based on amino acid similarity with MUSCLE
165 (Edgar 2004) as implemented in SeaView (v. 4.5.4; Gouy et al. 2010). We then
166 checked each sequence by eye and manually trimmed them to the length of the
167 shortest region observed among the four species. As we are examining the
168 relationship between three focal species and an outgroup, a missing species for a
169 genetic region would have limited utility for phylogenetic inferences. We made no
170 effort to identify specific genes within these datasets, with the exception of Na^+,K^+-

171 ATPase which we located in our *de novo* assemblies for each species using Blast (see
172 above).
173
174 *Species trees*
175 We first concatenated all aligned mtDNA regions into a single dataset (i.e. no
176 partitioning between regions). With jModelTest 2 (v. 2.1.7, Guindon and Gascuel
177 2003; Darriba et al. 2012), we determined that a the generalized time reversible
178 model (GTR; Tavaré 1986), with a gamma distribution of rate heterogeneity best fit
179 this data based on AIC score (i.e. GTR + Γ model). We also concatenated all loci into
180 single alignments (i.e. no partitioning between genes) independently for both
181 nuclear gene datasets (reference-mapped and *de novo*-assembled). As above, we
182 used jModelTest 2 to determine the best-fitting mutation model. For both genomic
183 datasets, the best fit was GTR model with a proportion of invariable sites and a
184 gamma distribution of rate heterogeneity (i.e. GTR + I + Γ model). Finally, we
185 examined the topology of Na^+,K^+-ATPase using our *de novo* assemblies of this gene
186 for each species. In this case the GTR + Γ model best fit the data.
187 For all datasets, we independently produced maximum likelihood
188 phylogenies in RAxML (v. 8.1.7, Stamatakis 2014) with 100 bootstrap replicates for
189 each of the three possible topologies among the *Danaus* species. The site log
190 likelihoods from RAxML were used to perform the approximately unbiased (AU)
191 test implemented in CONSEL 0.2 (Shimodaira and Hasegawa 2001). Two trees were
192 statistically different from one another if $p \leq 0.05$.
193

194 *Discordance among nuclear gene trees*

195 To quantify the extent of phylogenetic discordance among our nuclear genes,
196 we employed Bayesian concordance analysis (BCA), as implemented in BUCKy (v.
197 1.4.3, Larget et al. 2010), to determine what proportion of genes concur with the
198 primary species tree, and what proportions support the two alternative
199 phylogenetic relationships (Ané et al. 2007). While BUCKy can identify significant
200 levels of gene-tree discordance, it does not differentiate between ILS and
201 hybridization to explain this discordance (Larget et al. 2010).

202 To carry out the BCA, we first produced individual trees for each gene in the
203 dataset of *de novo*-assembled transcripts using MrBayes (v. 3.2.2, Ronquist and
204 Huelsenbeck 2003), with two independent runs of 10^7 generations and a "burn in"
205 period of 10^5 generations. Rather than *a priori* selecting a mutation model for each
206 gene, we used the reversible-jump Markov chain Monte Carlo approach as described
207 by Huelsenbeck and colleagues to examine the parameter space for each locus and
208 find the best set of parameters for that particular dataset (Huelsenbeck et al. 2004).

209 We combined each of the two independent MrBayes runs for each gene using
210 the mbsum command in BUCKy (v. 1.4.3, Larget et al. 2010). With the combined
211 files, we examined the extent of discordance as measured by the sample-wide
212 concordance factor (CF). This measure indicates the proportion of gene trees that
213 support a particular species tree. The data was analyzed using an α prior of 1. α is an
214 *a priori* discordance parameter that indicates the expected level of discordance
215 among the different genes being analyzed (ranging from 0 to ∞; Larget et al. 2010).
216 If there is no expected discordant topologies among gene trees, then α=0, whereas

217 $\alpha=\infty$ indicates that all gene trees are expected to have independent topologies. In
218 our analysis, other values of α (0.1 & 10) did not greatly alter inferred levels of
219 incongruence (SI Table 3).
220
221 *Differentiating between incomplete lineage sorting and genetic introgression*
222 While BUCKy analysis reveals the extent of nuclear discordance among taxa,
223 it does not indicate whether observed discordance is more likely to be due to ILS or
224 genetic introgression after species splitting (although these are not mutually
225 exclusive). To examine these two hypotheses we employed the ABBA/BABA test to
226 calculate Patterson's D statistic for our dataset (Green et al. 2010). This statistic uses
227 comparisons between three focal samples and an outgroup to determine whether
228 phylogenetically-informative sites are in agreement with the primary phylogeny
229 (AABB sites), or else support one of the two possible alternative relationships
230 (ABBA or BABA, respectively). If incomplete lineage sorting is the primary
231 contributor to observed phylogenetic incongruence, then ABBA and BABA sites
232 should be present in approximately equal frequencies (D statistic ≈ 0). However,
233 genetic exchange that occurs after splitting may result in an excess of either ABBA
234 or BABA sites (D statistic $\neq 0$). Structure in the ancestral population could also
235 produce an asymmetry in ABBA/BABA sites, whereas post-splitting, symmetrical
236 genetic exchange could produce equal frequencies of sites (Durand et al. 2011).
237 The ABBA/BABA test was performed with all informative sites, 4-fold
238 synonymous sites and 0-fold replacement sites from our 478 *de novo*-assembled
239 gene set. The standard deviation of D was determined by block jackknife sampling

(Kunsch 1989) with a block size of 40 genes, giving us 12 independent block estimates of D. 95% confidence intervals based on this jackknifed dataset were used to assess if D differed significantly from 0.

Genetic diversity and divergence times

ILS is most likely to be observed when multiple speciation events occur in rapid succession. Therefore, we wanted to estimate approximate splitting times for these species. However, changes in the effective population size of a species (N_e) over time can influence divergence estimates and patterns of evolution (Charlesworth 2009). Therefore, we examined relative differences in contemporary N_e for each species by calculating 4-fold synonymous genetic diversity (π_{4f}, Nei and Li 1979) within each of the four individual, wild-caught samples. To do this, we first mapped our trimmed reads to the species specific, *de novo*-assembled transcriptome for each of the four butterflies. We then used the HaplotypeCaller utility in the program GATK to identify genetic variants (McKenna et al. 2010). After this, sites with a read depth <30 were filtered out of the dataset. Likely coding sequences were determined by independently comparing each of the four species' *de novo* assembled transcriptomes to the set of *D. plexippus* predicted proteins (Dp_geneset_OGS2_pep.fasta, http://monarchbase.umassmed.edu/resource.html), using Blast with a translated nucleotide query ('blastx'; Altschul et al. 1990) and a minimum e value of 1e-50.

Using a custom Perl script, we calculated mean genetic diversity per gene for all 4-fold synonymous sites (π_{4f}) using the formula: (n/n-1) 2p(1-p), where n is the

number of chromosomes in the sample (here, n = 2) and p and (1-p) are the frequencies of alleles observed at a given site (here, either 1 & 0 [homozygous sites] or 0.5 & 0.5 [heterozygous site]). For each species, mean π_{4f} across all genes and 95% confidence intervals were estimated by bootstrap sampling each gene set 1,000 times with replacement, weighted by the number of 4-fold synonymous sites observed in each gene.

Species splitting times (t) can be roughly calculated using the formula $t = dS - \pi/2\mu$, where dS is an estimate of the average number of synonymous nucleotide differences per synonymous site observed between two species (Nei 1987), π is a measure of intraspecific diversity, and μ is an estimate of the mutation rate (Hudson et al. 1987; Bachtrog et al. 2006). For each species pair we estimated dS for all synonymous sites with the method of Nei and Gojobori (1986) as implemented in PAML (v. 4.8; Yang 2007). For our estimate of π, we used the larger of the species' π_{4f} estimates from each species pair (Table S4, following Bachtrog et al. 2006). No estimates of a mutation rate for *Danaus* butterflies have been made, so we used a recent, experimentally determined per generation estimate from *Heliconius melpomene* for our calculations (2.9×10^{-9} per site, Keightley et al. 2015). Both *Danaus* and *Heliconius* species are in the Nymphalidae family of butterflies. This per generation mutation estimate was converted to a per year estimate ($\mu = 1.45 \times 10^{-8}$), conditioned on five generations per year (Malcolm et al. 1987).

We additionally employed a Bayesian method to examine approximate species' splitting times. As there are no known fossils that would allow us to independently calibrate any of the nodes in our phylogeny, we employed a rate-

286 based estimate of evolution at neutral sites following methods described by Obbard
287 and colleagues (Obbard et al. 2012). For evaluation of neutral evolution, we utilized
288 all 4-fold synonymous sites from the concatenated dataset of our *de novo*
289 assemblies. While mutations at these sites may not be entirely neutral due to
290 processes such as codon usage bias (Hershberg and Petrov 2008) and other types of
291 selection (Lawrie et al. 2013), they are the best available option in this dataset.
292 Because we concatenated all 4-fold synonymous sites from each gene into a
293 single dataset, we did not take into account variation in evolution rates between
294 genes. Rather, we used the estimated 95% confidence intervals of the mutation rate
295 given for *H. melpomene* to produce a lognormal distribution of rate variation around
296 the mean for the complete dataset (6.5×10^{-9} - 2.8×10^{-8} changes per year, again
297 conditioned on five generations per year [Malcolm et al. 1987]). This allowed us to
298 partially capture potential variation in rates among branches and may reduce
299 overestimating the length of shorter branches (Schwartz and Mueller 2010).
300 We ran two MCMC chains of 10^8 iterations in the program BEAST (v. 1.8.1,
301 Drummond and Rambaut 2007), with a log-normal relaxed molecular clock. Our
302 substitution model was that of Hasegawa, Kishino and Yano (HKY, Hasegawa et al.
303 1985), with a proportion of invariant sites and a gamma distribution of rate
304 heterogeneity. We used a starting tree that matched the one found in our previous
305 analyses based on nuclear genes (Fig. 1B-D), with a birth-death process of lineage
306 birth as our tree prior (Gernhard 2008). Our "burn in" period was the initial 10% of
307 states, and parameters were logged every 1,000 iterations. LogCombiner was used
308 to merge our two separate runs (v. 1.8.1, included with the BEAST package). The log

309 files were checked using Tracer (v. 1.6; Rambaut et al. 2014) to ensure that an
310 effective sampling size (ESS) greater than 200 were achieved for each parameter.
311 Divergence times were estimated based on the 95% highest posterior density (HPD)
312 interval.
313
314 **Results**
315 *Phylogenic analysis*
316 Previous studies based on morphology and limited genetic data concluded
317 that *D. eresimus* and *D. gilippus* are more closely related to one another than either is
318 to *D. plexippus* (Ackery and Vane-Wright 1984; Lushai et al. 2003; Smith et al. 2005;
319 Brower et al. 2010). Here, we re-evaluated this conclusion using multiple datasets of
320 nuclear coding sequences, as well as mitochondrial data. The mitochondrial dataset
321 totaled 6,648 aligned nucleotides. The reference-mapped, nuclear gene dataset
322 contained 471 sequences, totaling 62,646 nucleotides, with an average sequence
323 length of 133 nucleotides. The *de novo* assembled nuclear gene dataset contained
324 478 sequences, totaling 220,188 nucleotides, with an average sequence length of
325 461 nucleotides. All datasets were limited in the total number of genes analyzed as
326 overlapping regions in each gene had to be assembled or mapped in all four species
327 for inclusion.
328 In contrast to previous findings (Lushai et al. 2003; Smith et al. 2005, Brower
329 et al. 2010), the best-supported mtDNA tree suggested that *D. plexippus* and *D.*
330 *gilippus* are sister taxa and *D. eresimus* is basal to them (Fig. 1A). However, the log

likelihoods of the three possible mtDNA trees were not significantly different from each other (Table 1) and the bootstrap support for this relationship was only 65%.

For both the reference-mapped and *de novo*-assembled datasets, the best-supported topology placed *D. plexippus* and *D. eresimus* as sister taxa, with *D. gilippus* a more distant relative (Fig. 1B & C). For the reference-mapped dataset, a relationship that places *D. eresimus* and *D. plexippus* as sister taxa was significantly better than the other two possible topologies, whereas the relationship that places *D. plexippus* and *D. gilippus* as sister taxa was significantly better than the relationship that placed *D. gilippus* and *D. eresimus* as sister taxa (Table 1). For the *de novo* assembled dataset, the two alternative topologies were significantly worse fits than the primary tree, but they were not significantly different from each other (Table 1). There was 100% bootstrap support for the best tree topology in both analyses utilizing nuclear gene datasets.

The major difference between the trees produced by the two nuclear gene datasets (reference-mapped vs. *de novo*-assembled) is in the estimated branch lengths. Specifically, the branch lengths are substantially shorter in the reference-mapped dataset, especially for the ancestral *Danaus* branch and that of the outgroup, *L. halia*. We attribute these differences to a bias towards highly conserved genes in the reference-mapped dataset (Hornett and Wheat 2012). Such bias becomes more problematic as the evolutionary distance between two species increases. Additionally, for all four species, fewer reads mapped to the *D. plexippus* reference than to each species' independently assembled *de novo* transcriptome (SI Table 2), and the average sequence length was shorter. For these reasons, in

354 subsequent analyses, we exclusively used the data from our *de novo*-assembled
355 dataset.

356 For Na^+,K^+-ATPase, the tree topology of this gene matched that observed
357 from the full gene datasets (Fig. S2). However, species' branch lengths for this gene
358 were much shorter than in the full datasets and bootstrap support for this
359 relationship was only 58%. Furthermore, this topology was not statistically better
360 than either of the alternative topologies (Table 1). These observations indicate that
361 this gene is highly conserved between these butterflies.

362

363 *Phylogenetic discordance*

364 We carried out an analysis of gene tree discordance using BUCKy. This
365 analysis revealed that the primary concordance tree was the same as that
366 determined in the maximum-likelihood analyses using the reference-mapped and *de*
367 *novo*-assembled concatenated, genomic datasets (Fig. 1D). However, the BUCKy
368 analysis also revealed significant discordance (>5%) between individual gene trees
369 and the inferred species tree. A higher proportion of genes supported a closer
370 relationship between *D. gilippus* and *D. plexippus*, than between *D. gilippus* and *D.*
371 *eresimus*.

372 The full dataset contained 5,735 informative sites for the ABBA/BABA test.
373 The percentages of sites supporting each of the three possible relationships are
374 given in Fig. 2. The D statistic for this data was -0.118 (95% CIs: -0.121 to -0.114).
375 There were 4,869 4-fold synonymous sites in our reduced dataset. For this data, the

D statistic was -0.134 (95% CIs: -0.138 to -0.130). There were 866 0-fold, non-synonymous sites. The D statistic was -0.025 (95% CIs: -0.031 to -0.019).

For all classes of sites, the D statistic was significantly less than 0, indicating that ABBA and BABA sites were not equally represented. In all cases, this was due to a larger number of BABA sites than ABBA sites. This suggests that a greater amount of gene flow has occurred between *D. plexippus* and *D. gilippus* after splitting than between *D. eresimus* and *D. gilippus*. It is also possible that this result is due to structure in the ancestral populations of these species (Green et al. 2010).

Genetic diversity and divergence time estimates

As rapid radiation increases the likelihood that ILS will occur between species (Whitfield and Lockhart 2007), we wanted to calculate the divergence times of these *Danaus* butterflies. However, a species' effective population size (N_e) can influence substitution rates (Ohta 1993; Woofit 2009), which could impact divergence time estimates. To assess the relative contemporary N_e of these species, we compared levels of 4-fold synonymous site diversity ($\pi_{4f,}$ Table 2). Of the four species, *D. eresimus* had the lowest synonymous diversity (π_{4f} = 0.010, 95% CIs: 0.009 - 0.011). The other three species all had similar levels of diversity (*L. halia*: π_{4f} = 0.022, 95% CIs: 0.021 - 0.023; *D. gilippus*: π_{4f} = 0.021, 95% CIs: 0.018 - 0.023; *D. plexippus*: π_{4f} = 0.021, 95% CIs: 0.021 - 0.022). As the *D. eresimus* dataset had fewer assembled transcripts (Table S2), we subsampled our *D. plexippus* dataset 10,000 times to calculate a mean and confidence intervals with the same number of genes as in the *D. eresimus* dataset. Our subsampled estimate of diversity for *D. plexippus*

399 was significantly different from that of *D. eresimus* (π_{4f} = 0.021, 95% CIs: 0.020 -
400 0.022), indicating that the lower diversity level of *D. eresimus* is not likely due to the
401 smaller number of genes represented in this dataset.

402 The similarities in genetic diversity levels exhibited in *D. plexippus* and *D.*
403 *gilippus* suggest that they have comparable contemporary N_e, while the population
404 from which the *D. eresimus* sample was collected likely has a relatively smaller N_e.
405 Differences in N_e between these species could affect estimates of divergence times.
406 Specifically, *D. eresimus* may have had a higher rate of evolution over time than the
407 other three species. However, Tajima's relative rate test (Tajima 1993), using all
408 sites from the concatenated *de novo* dataset suggests that *D. eresimus* has had a
409 similar rate of evolution to *D. gilippus* (χ^2 = 2.46, p=0.074), whereas the rate of
410 evolution in *D. plexippus* was higher than both *D. gilippus* (χ^2 = 31.11, p<0.001) and
411 *D. eresimus* (χ^2 = 20.25, p<0.001). Thus, we do not infer any evolutionary patterns in
412 relation to contemporary N_e in these species.

413 The estimate of pairwise synonymous divergence (dS) between *D. gilippus*
414 and *D. eresimus* was 0.369 (95% CIs: 0.348 – 0.390). Assuming five generations per
415 year (Malcolm et al. 1987), we estimated that the splitting time for *D. gilippus* and *D.*
416 *eresimus* was 11.7 million years ago (MYA), (95% CIs: 11.0 – 12.4 MYA). For *D.*
417 *gilippus* and *D. plexippus*, dS=0.312 (95% CIs: 0.310 – 0.337), and the estimated
418 splitting time was 10.4 MYA (95% CIs: 9.7 – 10.8 MYA). The difference between
419 these two divergence time estimates involving *D. gilippus* may reflect the larger
420 extent of post-splitting genetic exchange that we infer to have occurred between *D.*
421 *gilippus* and *D. plexippus*. It may also reflect a greater number of fixed differences

422 driven by the relatively smaller N_e of *D. eresimus*. Synonymous divergence between
423 *D. plexippus* and *D. eresimus* was 0.233 (95% CIs: 0.224 – 0.242), and our estimate of
424 the splitting time between these species was 7.1 MYA (95% CIs: 6.8 – 7.4 MYA).
425 Bayesian estimates of divergence times using 4-fold synonymous sites and a
426 log-normally distributed mutation rate suggested that *D. plexippus* and *D. eresimus*
427 diverged 7.2 MYA (95% highest posterior density [HPD]: 6.9 – 7.5), whereas *D.*
428 *gilippus* diverged from the common ancestor of *D. plexippus* and *D. eresimus* 11.0
429 MYA (95% HPD: 10.7 – 11.4). These estimates of splitting time are nearly identical
430 to our simple estimates, which were also based on synonymous divergence and a
431 fixed mutation rate. The simple divergence time estimate for *D. plexippus* and *D.*
432 *eresimus* based on observed synonymous divergence falls within the 95% HPD
433 interval for the divergence time between these species in the Bayesian analysis. The
434 HPD interval for the divergence time of *D. gilippus* and the *D. plexippus*/*D. eresimus*
435 common ancestor is somewhat lower than the simple estimate for the split between
436 *D. gilippus* and *D. eresimus*, but somewhat higher than the estimate for that between
437 *D. gilippus* and *D. plexippus.* Overall, these divergence estimates suggest that the
438 three species diverged relatively rapidly from one another (within 3 – 4 million
439 years), which may have increased the likelihood that ILS occurred.
440 We explicitly examined the extent of ILS given our estimated divergence
441 times by simulating the coalescent of 10,000 genes in *ms* (Hudson 2002). We used
442 0.02 for our estimate of θ ($4N_e\mu$) and converted our estimated divergence times to
443 units of $4N_e$ generations (run command: ms 3 10000 -t 0.02 -I 3 1 1 1 -ej 2.4 1 2 -ej
444 3.6 2 3 –T). From these simulations, we infer that ~8% of genetic regions will

445 exhibit an alternative topology to that of the true species relationship given the
446 divergence times calculated here.
447
448 **Discussion**
449 Evolutionary relationships within the *Danaus* genus are a subject of
450 uncertainty due to incongruences in both morphology and genetic sequences
451 (Ackery and Vane-Wright 1984; Kitching 1985; Brown et al. 2004; Smith et al. 2005;
452 Zhen et al. 2012). In contrast to previous studies (Ackery and Vane-Wright 1984;
453 Lushai et al. 2003; Smith et al. 2005; Brower et al. 2010), the analyses described
454 here indicate that *D. plexippus* and *D. eresimus* are the more closely related species,
455 whereas *D. gilippus* is a more distant relative. While this relationship is well
456 supported, we also observe significant phylogenetic discordance between these
457 species. This may be attributed to several factors including incomplete lineage
458 sorting (ILS) and post-speciation gene flow. Relative to the amount of evolutionary
459 divergence that occurred after these three species split from their common
460 ancestor, their speciation times are brief. This means that ILS is likely to explain
461 some phylogenetic incongruence. Using coalescence simulations, we calculated that
462 ~8% of gene regions will exhibit an alternative topology to that of the true species
463 tree given our estimated splitting times. This is less than the ~18% of phylogenetic
464 discordance detected. This observation, combined with the results of the
465 ABBA/BABA test, suggests that genetic exchange after these species diverged also
466 likely contributed to incongruences between these species. Similar explanations
467 have been proposed to explain extensive phylogenetic discordance in many other

468 species groups (e.g. Moody and Rieseberg 2012; Cui et al. 2013; Liu et al 2015),
469 including butterflies (Kozak et al. 2015).

470 In addition to amending current phylogenetic understanding of the *Danaus*
471 genus, our results shed light on the origins of the N122H substitution in the H1-H2
472 extracellular domain of Na^+,K^+-ATPase. As the gene tree topology for this region is
473 concordant with the best-supported phylogeny from whole nuclear gene datasets
474 (Fig. S2), the most parsimonious scenario to explain the N122H mutation in both *D.*
475 *plexippus* and *D. eresimus* is an emergence in their shared common ancestor. If this is
476 the case, it then either fixed before their split, or else fixed independently in each
477 lineage (Fig. S3A). It is also possible that the N122H mutation arose in the common
478 ancestor of all three *Danaus* species, and was subsequently lost in *D. gilippus* (Fig.
479 S3B). We cannot confidently differentiate between this and the previous hypothesis
480 with the data currently available.

481 If the N122H allele had a strong adaptive advantage when it arose, it most
482 likely fixed rapidly. This would have resulted in a selective sweep, reducing genetic
483 diversity in this gene (Maynard Smith and Haigh 1974). Interestingly, 4-fold
484 synonymous diversity estimates for Na^+,K^+-ATPase in both *D. plexippus* and *D.*
485 *eresimus* are slightly higher than genome-wide estimates (Table 2). This suggests
486 that if a sweep occurred, it was not recent in either species' evolutionary history.

487 Estimated synonymous divergence (dS) between *D. plexippus* and *D. eresimus*
488 for Na^+,K^+-ATPase is 0.15, whereas the genome-wide estimate is 0.23. This
489 divergence estimate translates to a splitting time of ~5.4 MY for Na^+,K^+-ATPase,
490 which is less than the estimated splitting time for these two species based on the full

491 gene dataset. This observation lends support to the third hypothesis that adaptive
492 introgression from either *D. plexippus* or *D. eresimus* into the other species can
493 explain the presence of the N122H mutation in both butterflies (Fig. S3C). However,
494 had this occurred, we would predict that Na^+K^+-ATPase genetic diversity in one of
495 these species would be low relative to other genetic regions. As noted previous, we
496 actually observe relatively high levels of synonymous diversity in Na^+K^+-ATPase.
497 Additionally, in the case of adaptive introgression, divergence in this gene between
498 *D. plexippus* and *D. eresimus* should be low relative to other genes. While we do
499 observe this (Fig. S2, Fig. S4), Na^+K^+-ATPase divergence is low overall among all the
500 butterflies in this study. This suggests that the low level of Na^+K^+-ATPase divergence
501 between *D. plexippus* and *D. eresimus* is not the result of introgression, but rather
502 that this gene is highly conserved between these butterflies.

503 Another question this study raises is the origins of the extensive phenotypic
504 divergence observed in *D. plexippus.* Divergent traits of *D. plexippus* include changes
505 in wing size, color and mating strategy, as well as the establishment of long-distance
506 migration (Ackery and Vane-Wright 1984). Changes in wing coloration may have
507 arisen in response to selection for increased mimic resemblance with *Limenitis*
508 *archippus* (the viceroy), as these two butterflies are Müllerian mimics of one another
509 (Ritland and Brower 1991). Other behavioral and morphological shifts could have
510 occurred in response to the evolution of migratory behavior in *D. plexippus* (Wells et
511 al. 1993; Dockx 2007). It is interesting in this respect that recent work suggests all
512 contemporary monarch populations (including non-migratory ones) originated
513 from a North American migratory population (Brower et al. 2007; Zhan et al. 2014).

514 Changes in mating strategy, which could have arisen in connection with migratory
515 behavior, may also have produced some morphological changes (Ackery and Vane-
516 Wright 1984). The uniquely derived traits of *D. plexippus* have likely obscured
517 phylogenetic relationships between North American *Danaus* species and lead to the
518 different conclusions than the ones presented here. It is noteworthy in this regard
519 that Tajima's relative rate test (based on all sites) suggests that *D. plexippus* has
520 experienced a significantly higher rate of molecular evolution than the other two
521 *Danaus* species (see Results).

522 It is also of interest that in most previous genetic analyses of *Danaus* species
523 relationships, all *D. eresimus* samples and nearly all *D. gilippus* samples came from
524 the Cayman Islands (Lushai et al. 2003; Smith et al. 2005; Brower et al. 2010). It is
525 possible that these samples may have unique attributes (e.g. recent genetic
526 exchange, reduced N_e, etc.), and are not typical of their species more broadly. While
527 the samples in this study all came from continental North America, they may also
528 not accurately capture the genetic diversity patterns of these widespread butterflies.
529 More specifically, it is possible that either contemporary or ancestral population
530 structure could be confounding some of our results. Population structure within
531 species can generate genetic patterns that resemble those of hybridization between
532 species (Green et al. 2010; Eriksson and Manica 2012). Very little population
533 structure has been observed in *D. plexippus*, presumably due to their migratory
534 behavior and overall high mobility (Eanes and Koehn 1978, Brower and Boyce 1991,
535 Lyons et al. 2012). Less is known about population structure in *D. gilippus* or *D.*
536 *eresimus*. However, while not migratory like *D. plexippus*, both are also considered to

537 be highly mobile (Smith et al. 2002). In future work, we hope to address interesting
538 questions regarding gene flow and population structure within these butterflies
539 throughout their geographic ranges. We also hope to look across the *Danaus* clade
540 more broadly to assess levels of phylogenetic incongruence throughout this genus.
541
542 **Conclusions**
543 Common ancestry is the simplest explanation for the shared N122H mutation
544 in the H1-H2 extracellular domain of Na^+,K^+-ATPase observed in *D. plexippus* and *D.*
545 *eresimus*. However, earlier origins within *Danaus* or post-speciation genetic
546 exchange are also possibilities. Relatively rapid divergence and historical
547 introgression likely contributed to observed phylogenetic incongruences among
548 these North American *Danaus* butterflies. As the majority of phylogenetic analyses
549 for the milkweed butterflies (*Danaidae*) have relied heavily on morphology and
550 limited genetic data, this study highlights a potential need to reevaluate the
551 relationships among milkweed butterflies more broadly. In particular, the extent of
552 incomplete lineage sorting and genetic introgression in this clade should be
553 assessed. Such examinations could potentially reveal more about the evolution of
554 novel morphological and behavioral traits in these butterflies including *D. plexippus*.
555
556 **Acknowledgements**
557 V. Miró Pina and M. Schumer provided helpful comments on earlier versions of this
558 work. A Briscoe kindly contributed the *D. gilippus*, *D. eresimus* and *L. halia* for the
559 original study that produced the original data utilized here.

560

561

562 **Data Accessibility**

563 The data used for this study can be found at: http://genomics-pubs.princeton.edu

564 /insect_genomics/data.shtml

565

566 **References**

567 Aardema, M. L., Y. Zhen and P. Andolfatto. 2012. The evolution of cardenolide-
568 resistant forms of Na^+,K^+-ATPase in Danainae butterflies. Mol. Ecol. 21: 340-349.
569 Ackery, P. R. and R. I. Vane-Wright. 1984. Milkweed butterflies: their cladistics and
570 biology. Cornell Univ. Press, Ithaca, NY.
571 Agrawal, A. A., G. Petschnka, R. A. Bingham, M. G. Weber and S. Rasmann. 2012. Toxic
572 cardenolides: chemical ecology and coevolution of specialized plant–herbivore
573 interactions. New Phytol 194:28-45.
574 Ané, C., B. Larget, D. A. Baum, S. D. Smith and A. Rokas. 2007. Bayesian estimation of
575 concordance among gene trees. Mol. Biol. Evol. 24:412-426.
576 Altschul, S. F., W. Gish, W. Miller, E. W. Myers and D. J. Lipman. 1990. Basic local
577 alignment search tool. J. Mol. Biol. 215:403-410.
578 Baack, E. J. and L. H. Rieseberg. 2007. A genomic view of introgression and hybrid
579 speciation. Curr. Opin. Genet. Dev. 17:513-518.
580 Bachtrog, D., K. Thornton, A. Clark and P. Andolfatto. 2006. Extensive introgression
581 of mitochondrial DNA relative to nuclear genes in the *Drosophila yakuba* species
582 group. Evolution 60:292-302.

583 Brower, A. V. Z. and T. M. Boyce. 1991. Mitochondrial DNA variation in monarch
584 butterflies. Evolution 45:1281-1286.
585 Brower, L. P. and C. M. Moffit. 1974. Palatability dynamics of cardenolides in the
586 monarch butterfly. Nature 249:280-283.
587 Brower, L. P., K. S. Oberhauser, M. Boppré, A. V. Z. Brower and R. I. Vane-Wright.
588 2007. Monarch sex: ancient rites, or recent wrongs? Antenna 31: 12–18.
589 Brower, A. V. Z., N. Wahlberg, J. R. Ogawa, M. Boppré, and R. I. Vane-Wright. 2010.
590 Phylogenetic relationships among genera of danaine butterflies (Lepidoptera:
591 Nymphalidae) as implied by morphology and DNA sequences. Syst. Biodivers.
592 8:75-89.
593 Brown, K. S. Jr., B. von Schoultz and E. Suomalainen. 2004. Chromosome evolution in
594 Neotropical Danainae and Ithomiinae (Lepidoptera). Hereditas 141:216-236.
595 Charlesworth, B. 2009. Effective population size and patterns of molecular evolution
596 and variation. Nat. Rev. Genet. 10:195-205
597 Cui, R., M. Schumer, K. Kruesi, R. Walter, P. Andolfatto and G. G. Rosenthal. 2013.
598 Phylogenomics reveals extensive reticulate evolution in *Xiphophorus* fishes.
599 Evolution 67:2166-2179.
600 Darriba, D., G. L. Taboada, R. Doallo and D. Posada. 2012. jModelTest 2: more
601 models, new heuristics and parallel computing. Nat. Methods 9:772.
602 Degnan, J. H. and N. A. Rosenberg. 2006. Discordance of species trees with their most
603 likely gene trees. PLoS Genet. 2:e68.
604 Degnan, J. H. and N. A. Rosenberg. 2009. Gene tree discordance, phylogenetic
605 inference and the multispecies coalescent. Trends Ecol. Evol. 24:332-340.

606 Dobler, S., G. Petschenka and H. C. Pankoke. 2011. Coping with toxic plant
607 compounds - the insect's perspective on iridoid glycosides and cardenolides.
608 Phytochemistry 72:1593-1604.
609 Dobler, S., S. Dalla, V. Wagschal and A. A. Agrawal. 2012. Community-wide
610 convergent evolution in insect adaptation to toxic cardenolides by substitutions
611 in the Na,K-ATPase. Proc. Natl. Acad. Sci. USA 109:13040-13045.
612 Dobler, S., G. Petschnka, V. Wagschal, L. Flacht. 2015. Convergent adaptive evolution
613 – how insects master the challenge of cardiac glycoside-containing host plants.
614 Entomol. Exp. Appl. 157:30-39.
615 Dockx, C. 2007. Directional and stabilizing selection on wing size and shape in
616 migrant and resident monarch butterflies, *Danaus plexippus* (L.), in Cuba. Biol. J.
617 Linn. Soc. 92:605-616.
618 Drummond, A. J. and A. Rambaut. 2007. BEAST: Bayesian evolutionary analysis by
619 sampling trees. BMC Evol. Biol. 7:214.
620 Eanes, W.F. and R. K. Koehn. 1978. Analysis of genetic structure in the monarch
621 butterfly, *Danaus plexippus* L. Evolution 32:784–797.
622 Edgar, R. C. 2004. MUSCLE: multiple sequence alignment with high accuracy and
623 high throughput. Nucleic Acids Res. 32:1792-7197.
624 Eriksson, A. and A. Manica. 2012. Effect of population structure on the degree of
625 polymorphism shared between modern human populations and ancient
626 hominins. Proc. Natl. Acad. Sci. USA 109:13956-13960.
627 Gernhard, T. 2008. The conditioned reconstructed process. J. Theor. Biol. 253:769-
628 778.

629 Gouy, M., S. Guindon and O. Gascuel. 2010. SeaView version 4: a multiplatform
630 graphical user interface for sequence alignment and phylogenetic tree building.
631 Mol. Biol. Evol. 27:221-224.
632 Green, R. E., J. Krause, A. W. Briggs, T. Maricic, U. Stenzel, M. Kircher, N.Patterson, H.
633 Li, W. Zhai, M. H. Fritz, et al. 2010. A draft sequence of the Neanderthal genome.
634 Science 328:710–722.
635 Guindon, S. and O. Gascuel. 2003. A simple, fast and accurate method to estimate
636 large phylogenies by maximum-likelihood. Syst. Biol. 52:696-704.
637 Hasegawa, M., H. Kishino and T. Yano. 1985. Dating of the human-ape splitting by a
638 molecular clock of mitochondrial DNA. J. Mol. Evol. 22:160-174.
639 Hershberg, R. and D. A. Petrov. 2008. Selection on codon bias. Annu. Rev. Genet.
640 42:287-299.
641 Holzinger, F. and M. Wink. 1996. Mediation of cardiac glycoside insensitivity in the
642 monarch butterfly (*Danaus plexippus*): role of an amino acid substitution in the
643 ouabain binding site of Na^+,K^+-ATPase. J. Chem. Ecol. 22:1921-1937.
644 Hornett, E. A. and C. W. Wheat. 2012. Quantitative RNA-Seq analysis in non-model
645 species: assessing transcriptome assemblies as a scaffold and the utility of
646 evolutionary divergent genomic reference species. BMC Genomics 13:361.
647 Hudson, R. R. 2002. Generating samples under a Wright-Fisher neutral model of
648 genetic variation. Bioinformatics 18: 337-338.
649 Hudson, R. R., M. Kreitman and M. Aguadé. 1987. A test of neutral molecular
650 evolution based on nucleotide data. Genetics 116:153-159.

651 Huelsenbeck, J. P., B. Larget and M. E. Alfaro. 2004. Bayesian phylogenetic model
652 selection using reversible jump Markov chain Monte Carlo. Mol. Biol. Evol.
653 21:1123-1133.
654 Keightley, P. D., A. Pinharanda, R. W. Ness, F. Simpson, K. K. Dasmahapatra, J. Mallet,
655 J. W. Davey and C. D. Jiggins. 2015. Estimation of the spontaneous mutation rate
656 in *Heliconius melpomene*. Mol. Biol. Evol. 32:239-243.
657 Kozak, K. M., N. Wahlberg, A. Neild, K. K. Dasmahapatra, J. Mallet and C. D. Jiggins.
658 2015. Multilocus species trees show the recent adaptive radiation of the mimetic
659 Heliconius butterflies. Syst. Bio. 64:505-524.
660 Kunsch, H. 1989. The jackknife and the bootstrap for general stationary
661 observations. Ann. Stat. 17:1217-1241.
662 Larget, B. R., S. K. Kotha, C. N. Dewey and C. Ané. 2010. BUCKy: Gene tree/species
663 tree reconciliation with Bayesian concordance analysis. Bioinformatics 26:2910-
664 2911.
665 Lawrie, D. S., P. W. Messer, R. Hershberg and D. A. Petrov. 2013. Strong purifying
666 selection at synonymous sites in *D. melanogaster*. PLoS Genet. 9:e1003527.
667 Li, H., B. Handsaker, A. Wysoker, T. Fennell, J. Ruan, N. Homer, G. Marth, G. Abecasis,
668 R. Durbin and 1000 Genome Project Data Processing Subgroup. 2009. The
669 Sequence alignment/map (SAM) format and SAMtools. Bioinformatics 25:2078-
670 2079
671 Liu, K. J., E. Steinberg, A. Yozzo, Y. Song, M. H. Kohn and L. Nakhleh. 2015.
672 Interspecific introgressive origin of genomic diversity in the house mouse. Proc.
673 Natl. Acad. Sci. USA 112:196-201.

674 Lunter, G. and M. Goodson. 2011. Stampy: a statistical algorithm for sensitive and
675 fast mapping of Illumina sequence reads. Genome Res. 21:936-939.
676 Lushai, G., D. A. S. Smith, D. Goulson, J. A. Allen and N. Maclean. 2003. Mitochondrial
677 DNA clocks and the phylogeny of *Danaus* butterflies. Insect Sci. Appl. 23:309-315.
678 Lyons, J. I., A. A. Pierce, S. M. Barribeau, E. D. Sternberg, A. J. Mongue and J. C. de
679 Roode. 2012. Lack of genetic differentiation between monarch butterflies with
680 divergent migration destinations. Mol. Ecol. 21:3433-3444.
681 Maddison, W. P. and L. L. Knowles. 2006. Inferring phylogeny despite incomplete
682 lineage sorting. Syst. Biol. 55:21-30.
683 Malcolm, S. B., B. J. Cockrell and L. P. Brower. 1987. Monarch butterfly voltinism:
684 effects of temperature constraints at different latitudes. Oikos 49:77-82.
685 Mallet, J., N. Besansky and M. W. Hahn. 2015. How reticulated are species? Bioessays
686 37: DOI 10.1002/bies.201500149.
687 Maynard Smith, J. and J. Haigh. 1974. The hitchhiking effect of a favourable gene.
688 Genet. Res. 23:23–35.
689 McKenna, A., M. Hanna, E. Banks, A. Sivachenko, K. Cibulskis, A. Kernytsky, K.
690 Garimella, D. Altshuler, S. Gabriel, M. Daly and M. A. DePristo. 2010. The Genome
691 Analysis Toolkit: a MapReduce framework for analyzing next-generation DNA
692 sequencing data. Genome Res. 20:1297-1303.
693 Moody, M. L. and L. H. Rieseberg. 2012. Sorting through the chaff, nDNA gene trees
694 for phylogenetic inference and hybrid identification of annual sunflowers
695 (*Helianthus* sect. *Helianthus*). Mol. Phylogenet. Evol. 64:145-155.
696 Nei, M. 1987. Molecular evolutionary genetics. New York: Columbia Univ. Press.

697 Nei, M. and W-H. Li. 1979. Mathematical model for studying genetic variation in
698 terms of restriction endonucleases, Proc. Natl. Acad. Sci. USA 76:5269-5273.
699 Nei, M. and T. Gojobori. 1986. Simple methods for estimating the numbers of
700 synonymous and nonsynonymous nucleotide substitutions. Mol. Biol. Evol. 3:418-
701 426.
702 Obbard, D. J., J. Maclennan, K-W. Kim, A. Rambaut, P. M. O'Grady and F. M. Jiggins.
703 2012. Estimating divergence dates and substitution rates in the *Drosophila*
704 phylogeny. Mol. Biol. Evol. 29:3459-3473.
705 Ohta, T. 1993. Amino acid substitution at the Adh locus of Drosophila is facilitated
706 by small population size. Proc. Natl. Acad. Sci. USA. 90:4548-51.
707 Petschenka, G., S. Fandrich, N. Sander, V. Wagschal, M. Boppré and S. Dobler. 2013.
708 Stepwise evolution of resistance to toxic cardenolides via genetic substitutions in
709 the Na+/K+-ATPase of milkweed butterflies (Lepidoptera: Danaini). Evolution
710 67:2753-2761.
711 Rambaut, A., M. A. Suchard, D. Xie and A. J. Drummond. 2014. Tracer v1.6, Available
712 from http://beast.bio.ed.ac.uk/Tracer.
713 Ritland, D. B. and L. P. Brower. 1991. The viceroy butterfly is not a batesian mimic.
714 Nature 350:497-498.
715 Ronquist, F., and J. P. Huelsenbeck. 2003. MrBayes 3: Bayesian phylogenetic
716 inference under mixed models. Bioinformatics 19:1572-1574.
717 Schulz, M. H., D. R. Zerbino, M. Vingron and E. Birney. 2012. Oases: Robust de novo
718 RNA-seq assembly across the dynamic range of expression levels. Bioinformatics
719 28:1086-1092.

720 Schwartz, R. S. and R. L. Mueller. 2010. Branch length estimation and divergence
721 dating: estimates of error in Bayesian and maximum likelihood frameworks. BMC
722 Evol. Biol. 10:5.
723 Shimodaira, H. and M. Hasegawa. 2001. CONSEL: for assessing the confidence of
724 phylogenetic tree selection. Bioinformatics 17: 1246-1247.
725 Smith, D. A. S., G. Lushai and J. A. Allen. 2005. A classification of *Danaus* butterflies
726 (Lepidoptera: Nymphalidae) based upon data from morphology and DNA. Zool. J.
727 Linn. Soc. 144:191–212.
728 Stamatakis, A. 2014. RAxML Version 8: A tool for Phylogenetic Analysis and Post-
729 Analysis of Large Phylogenies. Bioinformatics 30:1312-1313.
730 Stern, D. L. 2013. The genetic causes of convergent evolution. Nat. Rev. Genet.
731 14:751-764.
732 Tajima, F. 1993. Simple methods for testing the molecular evolutionary clock
733 hypothesis. Genetics 135:599-607.
734 Tavaré, S. 1986. Some Probabilistic and Statistical Problems in the Analysis of DNA
735 Sequences. Lectures Math. Life Sci. 17:57–86.
736 Wells, H., P. H. Wells and S. H. Rogers. 1993. Is multiple mating an adaptive feature
737 of monarch butterfly winter aggregation? Pp. 61-68. S. B. Malcolm and M. P.
738 Zalucki, eds. Biology and Conservation of the Monarch Butterfly. No. 38 Science
739 Series, Nat. Hist. Mus. of Los Angeles Co. Los Angeles, CA. USA.
740 Woofit, M. 2009. Effective population size and the rate and pattern of nucleotide
741 substitutions. Biol. Lett. 5:417-420.

742 Yang, Z. 2007. PAML 4: a program package for phylogenetic analysis by maximum
743 likelihood. Mol. Biol. Evol. 24: 1586-1591.
744 Zerbino, D.R. and E. Birney. 2008. Velvet: algorithms for de novo short read
745 assembly using de Bruijn graphs. Genome Res. 18:821-829.
746 Zhan, S., W. Zhang, K. Niitepõld, J. Hsu, J. F. Haeger, M. P. Zalucki, S. Altizer, J. C. de
747 Roode, S. M. Reppert and M. R. Kronforst. 2014. The genetics of monarch butterfly
748 migration and warning coloration. Nature 514:317-321.
749 Zhen, Y., M. L. Aardema, E. M. Medina, M. Schumer and P. Andolfatto. 2012. Parallel
750 molecular evolution in an herbivore community. Science 337:1634-1637.

Tables

Table 1. Comparison of the three possible phylogenetic relationships among the butterflies in this study for all mitochondrial (mtDNA) and genomic regions (gDNA). ["ref. mapped" = reference-mapped nuclear gene dataset; *"de novo"* = *de novo*-assembled nuclear gene dataset]. Significance between trees was determined using the AU test. See Materials and Methods for more details.

Dataset	Tree Comparison (see Fig. 2)	$\lvert \Delta \ln L \rvert$	p value from AU test
mtDNA	Tree A – Tree B	1.5	0.270
mtDNA	Tree A – Tree C	0.2	0.391
mtDNA	Tree B – Tree C	1.6	0.202
gDNA (ref. mapped)	Tree A – Tree B	267.4	<0.001*
gDNA (ref. mapped)	Tree A – Tree C	239.2	<0.001*
gDNA (ref. mapped)	Tree B – Tree C	30.3	0.024*
gDNA (*de novo*)	Tree A – Tree B	282.9	<0.001*
gDNA (*de novo*)	Tree A – Tree C	297.6	<0.001*
gDNA (*de novo*)	Tree B – Tree C	22.6	0.057
Na^+,K^+-ATPase	Tree A – Tree B	3.5	0.841
Na^+,K^+-ATPase	Tree A – Tree C	3.5	0.220
Na^+,K^+-ATPase	Tree B – Tree C	4.4	0.069

* indicates statistical significance at $p \leq 0.05$.

759 **Table 2.** Levels of 4-fold synonymous nucleotide diversity (π_{4f}) across all mapped 4-

760 fold synonymous sites, as well as π_{4f} for Na^+,K^+-ATPase.

Species	Number of mapped genes[1]	Total number of 4-fold synonymous sites[2]	Weighted 4-fold synonymous π[3] (95% CIs)	4-fold synonymous π of Na^+,K^+-ATPase
D. plexippus	4,185	507,661	0.0214 (0.0208 - 0.0221)	0.0271
D. eresimus	1,481	94,920	0.0099 (0.0090 - 0.0108)	0.0103
D. gilippus	1,139	71,442	0.0207 (0.0184 - 0.0230)	0.0156
L. halia	2,625	195,577	0.0220 (0.0208 - 0.0232)	0.0000

761

762 [1] These are genes that contain at least one 4-fold synonymous site with read

763 coverage of 30 or greater.

764 [2] The total number of 4-fold synonymous sites with 30 or greater read coverage.

765 [3] Based on estimates from mapped genes (column 2), weighted by the number of 4-

766 fold synonymous sites in each gene.

Figures

Figure 1. A) The best supported phylogenetic relationship as determined using mtDNA sequence data. Numbers indicate branch lengths. This tree topology had 65% bootstrap support. B) The best supported phylogenetic relationship produced from 471 reference-mapped nuclear gene sequences. Numbers indicate branch lengths. This tree topology had 100% bootstrap support. C) The best supported phylogenetic relationship as determined using data from 478 *de novo*-assembled nuclear gene sequences. Numbers indicate branch lengths. This tree topology had 100% bootstrap support. D) Levels of phylogenetic concordance/discordance between the best-supported species tree and individual gene trees. The red text and diagonal line indicates the level of discordance (with credibility intervals) that supports a closer relationship between *D. plexippus* and *D. gilippus* (with α = 1.0). The blue text and diagonal line indicated the level of discordance (with credibility intervals) that supports a closer relationship between *D. gilippus* and *D. eresimus* (with α = 1.0). **NOTE: Branch lengths in these trees (A-D) are not drawn to the same scale *between* trees.**

Figure 2. The percentages of ABBA/BABA informative sites that match the best-supported species tree (Tree A) and the two alternative trees for the three North American *Danaus* species in this study for either all 4-fold/0-fold sites (all), just 4-fold synonymous sites (syn.) or just 0-fold replacement sites (rep.). ('gili.' = *D. gilippus*, 'eres.' = *D. eresimus*, 'plex' = *D. plexippus*, 'hali' = *L. halia*).

789 **Figure 1.**

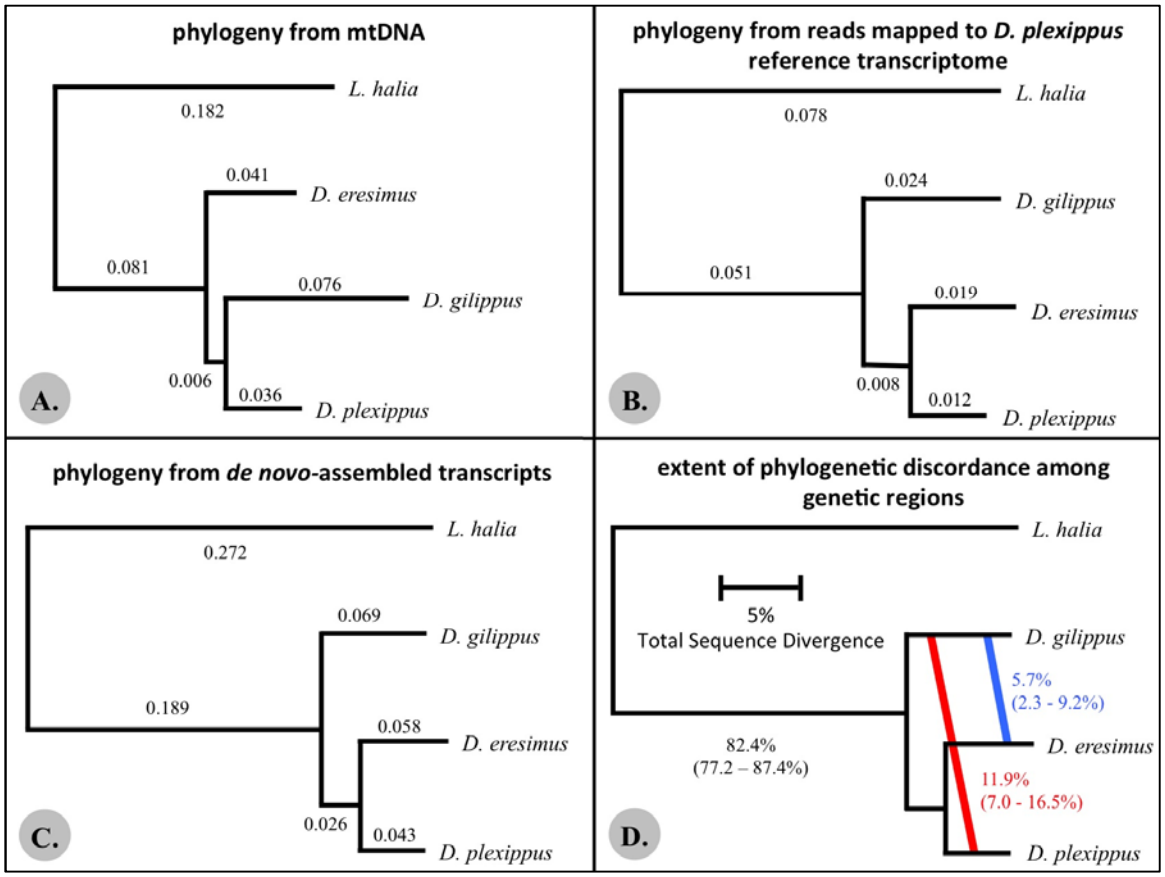

790

791

792 **Figure 2.**

Data type	Total informative sites	Tree A 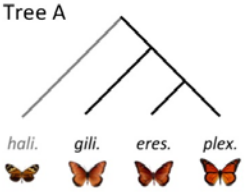 **AABB**	Tree B 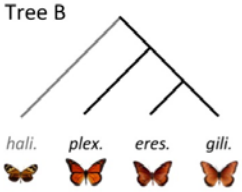 **ABBA**	Tree C 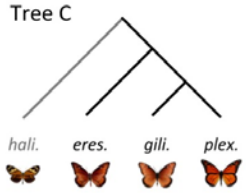 **ABAB** (BABA)
ABBA/BABA (all)	5735	2818 (41.7%)	1287 (22.4%)	630 (28.4%)
ABBA/BABA (syn.)	4869	2389 (49.1%)	1074 (22.1%)	1406 (28.9%)
ABBA/BABA (rep.)	866	2389 (49.1%)	213 (24.6%)	224 (25.9%)

793
794

795 **Supplementary Information**

796 **Table S1.** Summary statistics for the raw data used in this study, as well as the *de*

797 *novo* assembly of each species' transcriptome.

Species	Raw reads	Single-end (SE) or paired-end data (PE)?	Total nucleotides in *de novo* assembly	Number of transcripts in *de novo* assembly	N50 of *de novo* assembly
D. plexippus	28,266,296	SE	16,930,874	14,429	1,919
D. eresimus	5,878,381	PE	8,461,965	11,750	943
D. gilippus	1,738,243	PE	2,016,798	3,030	981
L. halia	16,067,453	SE	10,810,257	18,251	806

798

799 **Table S2.** The total number of Illumina reads for each species after quality
800 trimming, plus the number or trimmed reads that mapped to either the *D. plexippus*
801 CDS or a species-specific, *de novo* assembled transcriptome.

Species	Total trimmed reads	Reads mapped to *D. plexippus* reference CDS		Reads mapped to *de novo* assembled transcriptome	
D. plexippus	27,068,642	mapped	19,132,116	mapped	25,598,815
		percent	70.7%	percent	94.6%
D. eresimus	5,354,186 (pairs)	mapped	2,021,741	mapped	4,324,576
		percent	37.9%	percent	80.8%
D. gilippus	1,538,115 (pairs)	mapped	1,268,745	mapped	1,523,195
		percent	82.5%	percent	99.1%
L. halia	14,530,186	mapped	11,649,577	mapped	14,075,972
		percent	80.2%	percent	96.9%

802

803 **Table S3.** Percentage of gene trees that support each of the three alternative tree
804 topologies possible among the *Danaus* species in this study using an α prior of either
805 0.1, 1.0 or 10. Concordance factors (CF) are presented with creditability intervals (CI)
806 in parentheses.

Species Relationships	CF with α = 0.1 (CI)	CF with α = 1.0 (CI)	CF with α = 10.0 (CI)
Tree A (Fig. 2)	0.824 (0.772 - 0.874)	0.822 (0.770 - 0.872)	0.804 (0.753 - 0.851)
Tree B (Fig. 2)	0.057 (0.023 - 0.092)	0.058 (0.025 - 0.094)	0.069 (0.038 - 0.103)
Tree C (Fig. 2)	0.119 (0.070 - 0.165)	0.120 (0.075 - 0.165)	0.127 (0.086 - 0.172)

807

Supplementary Figures

Figure S1. Historical phylogeny (see Ackery and Vane-Wright 1984; Lushai et al. 2003; Smith et al. 2005; Brower et al. 2010) and amino acid sequences of the H1–H2 extracellular domain of the Na^+,K^+-ATPase gene in the *Danaus* species examined in this study, plus a second milkweed butterfly outgroup *Tirumala petiverana* (adapted from Aardema et al. 2012, Zhen et al. 2012). The presence of a Valine at position 111 (blue letters) in the three *Danaus* butterflies likely facilitates their ability to feed on milkweed and possibly sequester cardenolides. The N122H mutation (red letters) seen in *D. plexippus* and *D. eresimus* may also contribute to cardenolide feeding and sequestration ability (Zhen et al. 2012; Petschenka et al. 2013).

Figure S2. A.) The best supported phylogenetic relationship as determined using data from 478 *de novo*-assembled nuclear gene regions. Numbers indicate branch lengths (this is the same tree as shown in Fig. 1C). B.) The best supported phylogenetic relationship produced with data from the Na^+,K^+-ATPase gene (in RAxML with a gamma distribution of rate heterogeneity [i.e. GTR + Γ model]). This relationship has 58% bootstrap support based on 100 bootstrap replicates. The branches of these two trees are drawn to the same scale.

Figure S3. Graphical representation of potential scenarios to account for the presence of the N122H mutation in the H1-H2 extracellular domain of Na^+,K^+-ATPase in both *D. plexippus* and *D. eresimus*. Not all possible scenarios are displayed in this figure. A) The N122H mutation arose in the common ancestor of *D. plexippus*

831 and *D. eresimus* and either fixed in this common ancestor (right), or else fixed
832 independently in each linage (left). B) The N122H mutation arose in the common
833 ancestor of all three species, but was lost in *D. gilippus.* C) The mutation arose or
834 was present in either *D. plexippus* or *D. eresimus*, and then introgressed into the
835 second species. The dashed boxes are present to indicate that we cannot infer the
836 direction of this potential introgression, although our data suggests that if
837 introgression is responsible for this mutation in both species, then it is more
838 probably that it introgressed from *D. plexippus* into *D. eresimus*.
839
840 **Figure S4.** Comparison of log dS between *D. plexippus* and *D. eresimus* (x axis), and
841 log dS between *D. gilippus* and *L. halia* (y axis). The left figure shows dS estimates
842 based on the method of Nei and Gojobori (1986), as determined in PAML (v. 4.8;
843 Yang 2007). The right figure shows maximum-likelihood estimates of dS, also
844 determined in PAML. The single red dot in each figure indicates the location of the
845 dS estimates for the Na^+,K^+-ATPase gene. Solid lines indicate the regression line for
846 each dataset, and the dashed lines are the 95% confidence intervals for this line.

847 **Figure S1.**

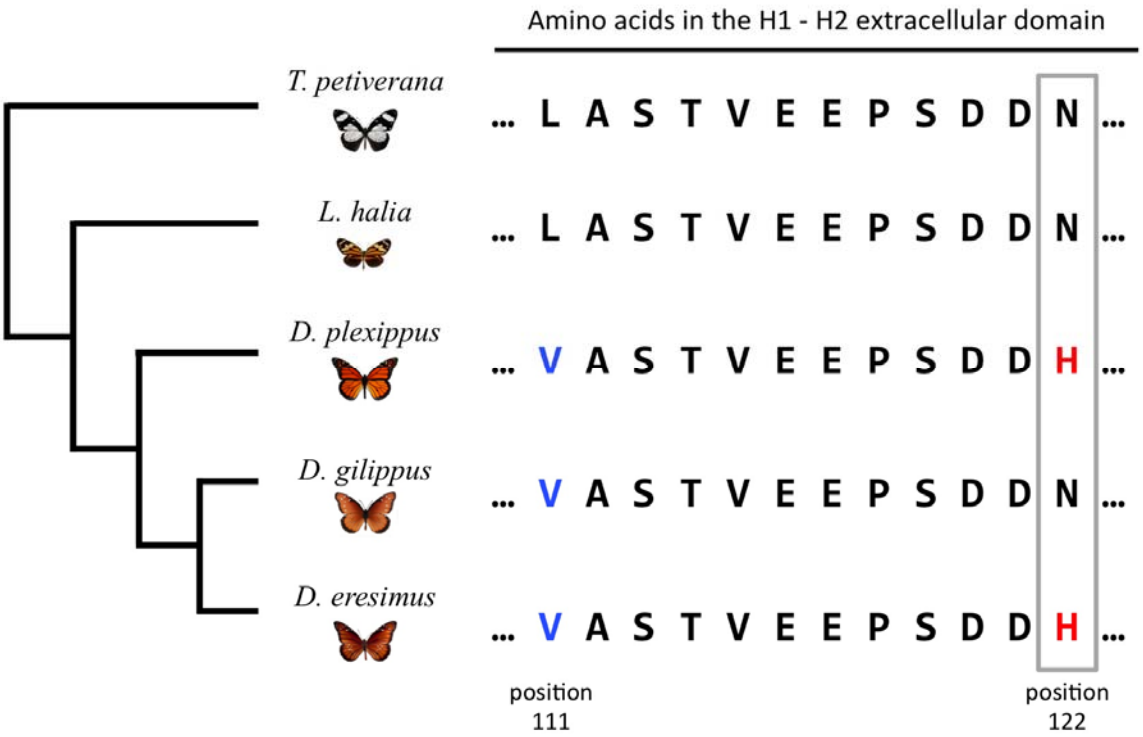

848

849 **Figure S2.**

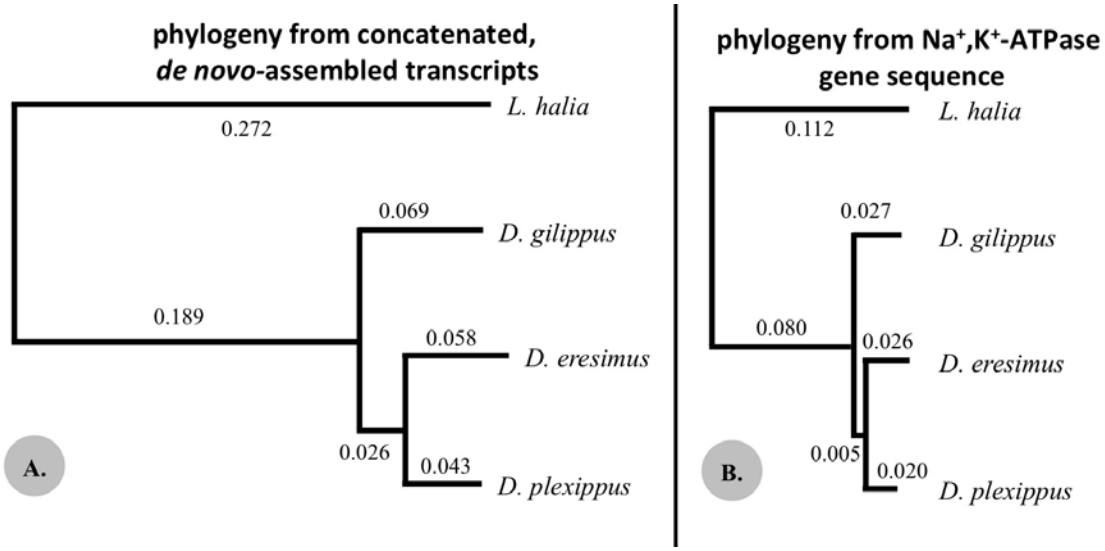

850
851

852 **Figure S3.**

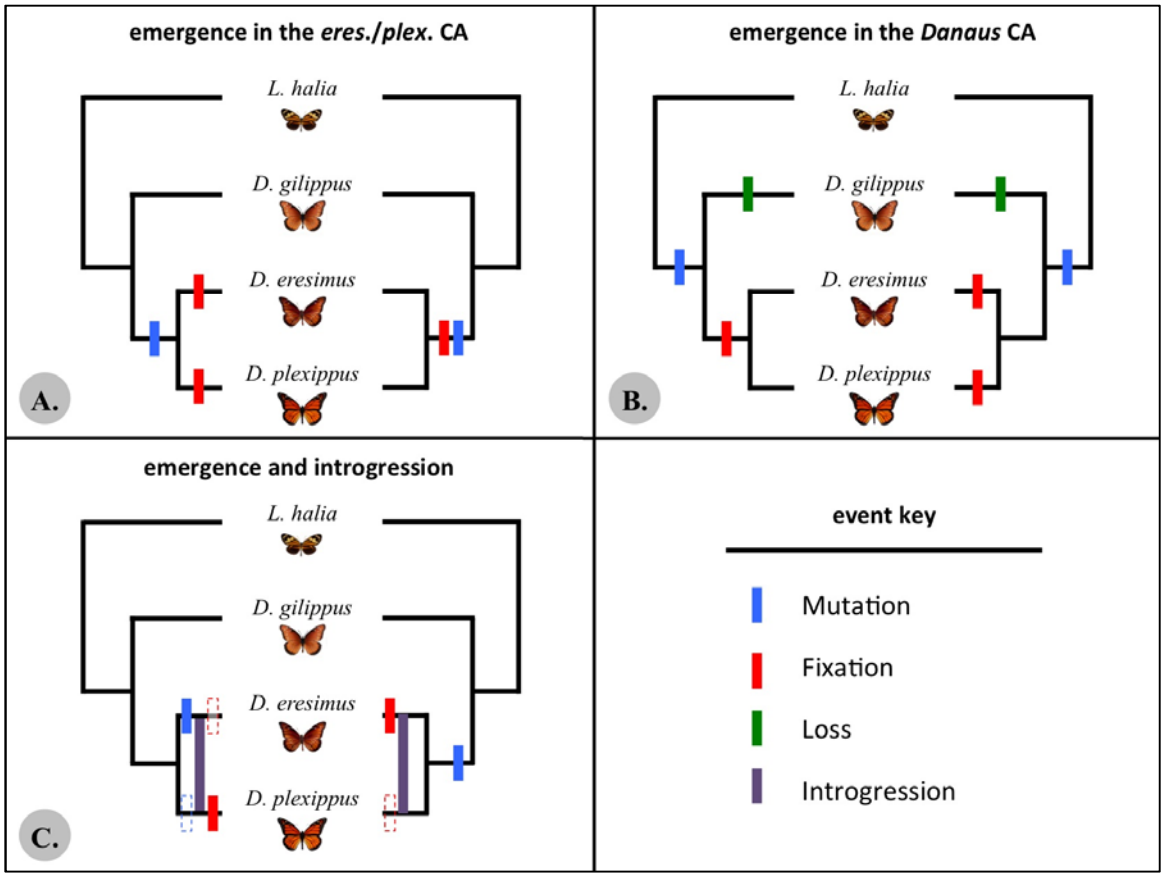

853

854

855 **Figure S4.**

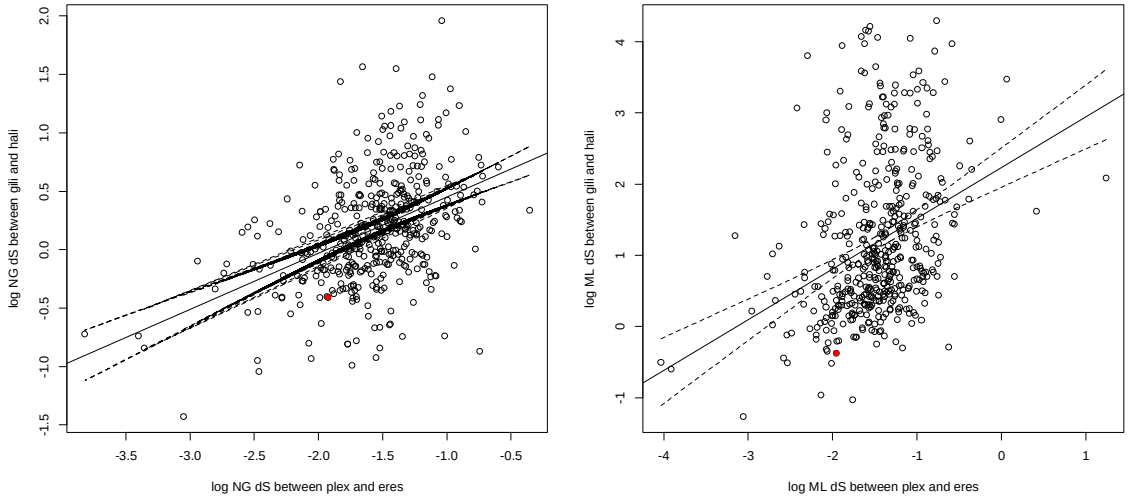

856

857